

1
2
3
4
5
6
7
8
9
10
11
12
13
14
15
16
17
18
19
20
21
22
23
24
25
26
27
28
29
30
31
32
33
34
35
36
37
38
39

Trait-based paleontological niche prediction demonstrates deep time parallel ecological occupation in specialized ant predators

Christine E. Sosiak¹, Tyler Janovitz², Vincent Perrichot³, John Paul Timonera⁴, Phillip Barden^{1,5}
1. Federated Department of Biological Sciences, New Jersey Institute of Technology; 2. Foundation Medicine Inc.; 3. Géosciences Rennes, Univ. Rennes, CNRS; 4. Biological Sciences Program, St. Mary's University; 5. Division of Invertebrate Zoology, American Museum of Natural History

Abstract

Understanding the paleoecology of species is fundamental to reconstructions of paleoecological communities, analyses of changing paleoenvironments, and the evolutionary history of many lineages. One method of establishing paleoecology is through comparing the morphology of extant analogs to extinct species; this method has been applied to many vertebrate groups using predictive linear models, but has been rarely applied using invertebrate taxa or non-linear frameworks. The ant fossil record, which frequently preserves specimens in three-dimensional fidelity, chronicles putative faunal turnover during the Late Cretaceous and into Cenozoic. The earliest fossil species comprise enigmatic stem-groups that underwent extinction concomitant with crown ant diversification. Here, we apply a wide-ranging extant ecomorphological dataset to demonstrate the utility of Random Forest machine learning classification in predicting the ecology of stem-group “hell ants”. We reconstruct a predicted ecomorphological assemblage of this phenotypically aberrant group of extinct ants, and compare predicted hell ant ecologies to the ecological occupations of their closest living analogs, lineages of solitary predators with highly specialized mandibular morphology. In contrast to previous hypotheses, we find that hell ants were primarily leaf litter or ground-nesting and foraging taxa, and that the ecological breadth of this unusual lineage mirrored that of living groups. Results suggest ecological coherence between the Mesozoic and modern communities, even as the earliest occupants of predatory niches were phylogenetically and morphologically distinct.

40 **Introduction**

41 Estimating the ecological niche occupation of extinct taxa is a central component of
42 paleontology. The putative ecologies of extinct organisms are routinely incorporated into
43 analyses of extinction risk, paleoenvironmental reconstruction, and lineage evolutionary
44 history (Palmqvist et al. 2003; Benson et al. 2014; Frederickson et al. 2018). Even as
45 aspects of extinct niche occupation may be reliably inferred by the preservation of
46 individual traits in fossil specimens, organismal ecology remains multifaceted.
47 Morphology frequently reflects ecology across entire phenotypes (Williams 1972; Losos
48 1992) and phenotypic syndromes may be linked to multiple aspects of an organism's
49 ecological niche spanning habitat, diet, and interactions. These ecologically-linked body
50 plans - ecomorphs - are found in such disparate taxa as fish, reptiles, arthropods, and
51 mammals (Barton et al. 2011; Gerry et al. 2011; Sanders et al. 2013; Figueirido et al.
52 2019). The relationship between ecological niche and multi-trait morphology can also be
53 leveraged to estimate paleoecologies. In lineages with surviving relatives, extant taxa
54 may serve as analogs for ecological niche estimation, however a partial fossil record
55 often reduces the utility of extant-to-extinct comparisons.

56
57 Across vertebrate species, limb anatomy is a predictor of locomotion, prey items, and
58 substrate behaviour. In particular, the forelimb anatomy of carnivores has been used to
59 predict the likely predatory habits and prey size of extinct carnivorous mammals and
60 mammaliaforms (Dunn et al. 2019; Ercoli et al. 2012; Figueirido et al. 2016; Jenkins et
61 al. 2020; Lungmus and Angielczyk 2021; Meloro and Louys 2014). Other examples of
62 extant morphology used in the prediction of extinct ecology include estimating prey type
63 in extinct raptor species from present-day birds of prey (Hertel 1995); predicting prey
64 items and modes of scavenging in extinct crocodyliforms from extant crocodyliform
65 snout morphology (Drumheller and Wilberg 2019); approximating arboreal behaviour in
66 extinct primates (Rector and Vergamini 2018); and predicting habitat preferences in
67 fossil *Anolis* lizards using ear canal shape (Dickson et al. 2017). In most cases,
68 potentially because of the difficulty of obtaining many complete skeletons, these
69 methods incorporate isolated body parts rather than full-body morphology; however,
70 morphometric analyses of mammalian skeletons have been used to predict the
71 locomotion mode of various Mesozoic mammaliaforms (Chen and Wilson 2015; Meng
72 et al. 2017).

73
74 Many attempts to predict paleoecology from extant morphology use techniques such as
75 canonical correlations analysis or canonical variate analysis, and in particular linear
76 discriminant analysis (Dickson et al. 2017; Dunn et al. 2019; Hertel 1995; Janis and
77 Figueirido 2014; Meloro and Louys 2014; Rector and Vergamini 2018). These methods
78 maximize variation in the measured traits between predetermined classes in

79 morphospace. The fossil specimen's most likely ecology is then determined by proximity
80 to each class mean in this constructed morphospace (Strauss 2010). These approaches
81 are powerful tools for establishing sets of traits most strongly associated with
82 predetermined classes, but are limited to linear relationships only among measured
83 traits, which may restrict accuracy by failing to incorporate non-linear predictive
84 relationships between traits.

85
86 While most predictive paleoecology studies have focused on vertebrate paleoecology,
87 minimal attention has been paid to these approaches in invertebrates, particularly
88 insects. Many extant insect lineages reach back to the Mesozoic or Paleozoic, and are
89 highly ecologically diverse. One example are the ants, which arose between ~150 and
90 100 Ma (Mega-annum) (Moreau et al. 2006; Brady et al. 2006; Borowiec et al. 2019).
91 With over 13,000 species comprising a significant component of terrestrial biomass,
92 ants are globally ubiquitous, speciose, and are present in most post-producer ecological
93 niches (Hölldobler and Wilson 1990). Importantly, despite this ecological diversity, ants
94 are also morphologically conserved with respect to broad bauplan functionality and
95 possess a rich fossil record extending back 100 Ma to the mid-Cretaceous. A majority of
96 ant fossils are known from fossil amber, which often preserves entire specimens with
97 high fidelity. Because of their well-defined homology and uniquely preserved fossil
98 history, extinct ants are strongly suited for testing paleoecological niche prediction
99 methods.

100
101 The earliest known ant fossils date to the Early–Late Cretaceous transition and
102 evidence extinct stem-lineages that began to diversify prior to the most recent common
103 ancestor of all living ants. Cretaceous fossils have fueled speculation on the ecological
104 occupation of the earliest ants because these taxa have bearing on the evolution of
105 eusociality more broadly. It was posited that these early species were unlikely to
106 construct nests, but instead used already-present cavities in soil and wood (Dlussky
107 1996; Wilson 1967; Wilson 1987a; Wilson 1987b; Grimaldi and Agosti 2000; Engel and
108 Grimaldi 2005). Based on their presumed wasp ancestors, they were additionally
109 argued to be predators (Dlussky 1996; Wilson 1987a; Wilson 1987b). As the taxonomic
110 diversity of extinct ant species increased, concordant with the discovery of new fossil
111 occurrences, paleoclimate reconstructions and contextualization with other fossils and
112 phylogenetic relationships suggested soil and leaf litter microhabitats in newly emerging
113 angiosperm forests (Wilson and Hölldobler 2005, Perrichot et al. 2008, Moreau et al.
114 2006, Moreau and Bell 2013). Phylogenetic reconstructions of extant lineages have
115 recovered ant ancestors as potentially hypogaeic soil-dwellers (Lucky et al. 2013).

116

117 Haidomyrmecines, or hell ants, are an enigmatic and highly specialized extinct
118 subfamily of ants comprising 16 described species and 10 genera (Perrichot et al.
119 2020). Hell ants occupy a stem-group position relative to modern ants and are
120 frequently recovered as sister to all other extinct and extant ants (Barden et al. 2016;
121 2020). They persisted throughout the mid-to-late Cretaceous as evidenced by amber
122 fossils ranging from 100 to 78 Ma on three different continents in Canada, Myanmar,
123 and France (Dlussky 1996; Perrichot et al. 2008; McKellar et al. 2013) and are
124 hypothesized to have undergone extinction concomitant with the diversification of extant
125 lineages. These ants are morphologically unique among the Formicidae in having
126 vertically-articulating mandibles, unlike the horizontal alignment of modern ants.
127 Remarkably, hell ants possess an array of horn-like cranial appendages that have been
128 directly observed to facilitate solitary predation through fossil remains (Barden et al.
129 2020): haidomyrmecines captured prey individually by articulating their mandibles
130 against their horns. Hell ants have been hypothesized as arboreal predators,
131 considering the potential difficulty of substrate manipulation with their vertically-aligned
132 mandibles, and frequent preservation in amber, potentially indicating close proximity to
133 tree resin (Dlussky 1996; Barden and Grimaldi 2012; Lattke and Melo 2020).

134
135 What functional niches did the earliest ant predators occupy and how does this
136 occupation compare with extant lineages? Here, we use a wide-ranging extant
137 morphometric dataset spanning over 160 species that has previously demonstrated a
138 quantitative link between morphology and ecology to predict the paleoecology of several
139 hell ant species. Using a supervised machine learning classification algorithm, Random
140 Forest, we predict foraging niche, nesting niche, and functional role for hell ants. With
141 these predictions, we reconstruct known ecomorphological space for haidomyrmecines
142 and compare these ecological occupations to those of extant lineages of specialized
143 solitary predators. Our results demonstrate repeated filling of functional niche space
144 across phylogenetically and morphologically distant lineages.

145

146 **Methods**

147 We applied a supervised machine learning approach by training multiple random forest
148 models on a comprehensive ecomorphological dataset of extant ant taxa. Briefly, for
149 each ecological niche aspect, we constructed a total of four overarching models trained
150 on four subsets of extant data to evaluate alternative predictive schemes based on body
151 size and dataset completeness in anticipation of partial fossil specimens: i) a complete
152 morphometric dataset comprising raw measurements; ii) a complete morphometric
153 dataset comprising size-corrected ratio measurements; iii) a subset of the complete
154 dataset comprising raw measurements; iv) a subset of the complete dataset comprising
155 size-corrected ratio measurements. We then used each model to predict ecological

156 niche aspects based on two alternate versions of input fossil data: one including
157 measurements based on assumed homology of haidomyrmine ants and another
158 assuming haidomyrmecine measurements corresponding with functional analogs of
159 extant ants. Niche aspects of each specimen were then predicted using the appropriate
160 model; the complete-dataset trained model for complete specimens, and subset-trained
161 model for incomplete specimens. All analyses were performed in R v.4.0.3 (R Core
162 Team, 2021).

163

164 ***Development of the predictive model***

165 *Training dataset*

166 We developed a predictive machine learning model using a training dataset of extant
167 ant morphometrics with sampling following Sosiak & Barden (2021). Our extant dataset
168 spans 15 subfamilies, 113 genera, and 167 species, including three specimens per
169 species where possible, and measuring as many conspecifics as were present in
170 museum collections otherwise. Polymorphic species are represented by the media
171 caste, and species with specialized castes are represented by non-specialized “minor”
172 workers. There is currently no evidence for specialized hell ant worker castes and
173 specialized worker castes are not a synapomorphy of crown ants.

174

175 Our morphometric sampling comprised linear measurements of 12 cephalic traits and
176 five post-cephalic traits. Most sampled traits have been previously linked to ecology
177 (Weiser and Kaspari 2006; Yates and Andrew 2011; Gibb et al. 2015; Yates et al.
178 2014). All measurements were conducted on point-mounted specimens under stereo
179 microscopy. Because body size in diverse species can drive the overwhelming majority
180 of variation in a dataset and potentially mask other important contributors, we created
181 two datasets: one comprising raw measurements and one comprising only size-
182 corrected ratios. A list of all traits measured with associated definitions may be found in
183 Supplementary Tables S1 and S2.

184

185 All specimens were assigned a binning from each of three ecological niche aspect
186 categories: functional role (six binnings), nesting niche (five binnings), and foraging
187 niche (four binnings). Specimen binnings were assigned based on literature surveys.
188 When any particular aspect of a species’ ecological niche was uncertain, the species
189 was assigned an “unknown” binning and excluded from further model development. We
190 collapsed the 35 observed combinations of niche binnings across all niche aspects into
191 10 ecomorph syndromes, defined after preliminary analysis indicated that some niche
192 combinations showed extensive morphological overlap. A list of all ecological niche
193 aspect binnings and syndromes with associated definitions may be found in

194 Supplementary Tables S3 and S4.

195

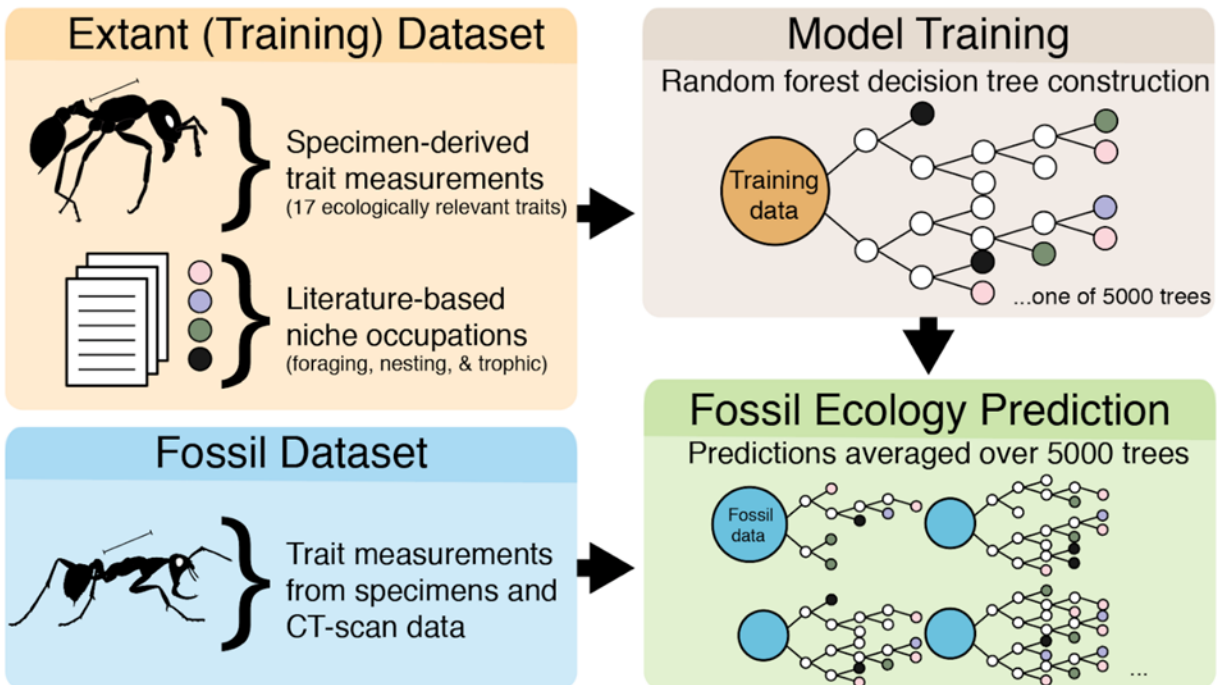
196 *Model development*

197 We implemented Random Forest analysis, a supervised machine learning algorithm, to
198 delimit species into ecological niches by morphology using our extant ant morphometric
199 dataset. Random Forest models are classification algorithms that partition morphospace
200 according to predefined ecological niche binnings through an assemblage of decision
201 trees (Breiman 2001). The algorithm builds a series of decision trees which each
202 provide a “vote” on a given specimen’s predicted category; the vote consensus from the
203 decision trees is then used as the final predicted category for the specimen. At each
204 split in each decision tree, a predetermined number of variables are randomly selected
205 and tested to evaluate their contribution to the accuracy of the model. During each
206 iteration of the model, one-third of the data is randomly removed and used to estimate
207 the error rate of that particular iteration; the converged test error rate across the
208 iterations is considered the out-of-bag error rate for the model. This removal of testing
209 data during bootstrapping eliminates the need for a priori separation of a testing and
210 training dataset, incorporating all collected data.

211

212 While other supervised machine learning or dimension reduction techniques have been
213 used in morphology-based paleoecological prediction, Random Forest has recently
214 been shown to outperform linear predictive approaches with respect to morphology
215 (Pigot et al. 2020; Sosiak & Barden 2021). This is the first application of Random Forest
216 in predicting extinct ecology to our knowledge. Random Forest models were trained on
217 our morphometric data, using both raw measurement datasets and size-corrected ratio
218 measurement datasets separately for each ecological niche aspect. We constructed
219 Random Forest models for functional role, nesting niche, foraging niche, and ecomorph
220 syndrome separately, allowing for both granular classification of ecological niche and
221 more synthesized classification. Model parameters were selected based on initial
222 sensitivity tests: mtry=4 (number of variables tested at each split) and ntree=5000
223 (number of trees iterated). Out-of-bag error rate estimates ranged from 15-22%,
224 reflecting accuracies of 78-85%; OOB error rates for each model are shown in Table
225 S5. All Random Forest analyses were implemented in the R package “randomForest”
226 (Liaw and Weiner 2018).

227



228

229 **Figure 1.** Diagrammatic workflow of predictive model development and testing. A
230 comprehensive morphometric dataset of extant ants was compiled; species were
231 binned according to various ecological niche aspects based on surveys of the literature.
232 Random Forest models were then trained on subsets of the original dataset.
233 Homologous traits were measured on fossil ant specimens; when available, traits were
234 measured from CT reconstructions, and otherwise were measured under light
235 microscopy. Finally, the pre-trained Random Forest models were used to predict extinct
236 ecology from fossil morphometric datasets.

237

238 *Fossil data*

239 We measured fossil hell ant specimens using a combination of stereo microscopy and
240 reconstructions of X-ray micro-computed tomography (micro-CT) scans. Twenty
241 specimens from 16 species and morphospecies were measured under stereo
242 microscopy. We submerged the amber specimens in water to reduce light distortion;
243 some measurements were not possible due to specimen positioning. Three specimens
244 were micro-CT scanned and reconstructed for subsequent measurements; two species
245 of hell ant and one species of *Pseudomyrmex macrops* from Dominican
246 to assess the reliability of CT-scan based data. Congeners of the Dominican
247 *Pseudomyrmex* fossil are extant today and their ecology is well consistent across the
248 genus and well-characterized. Two specimens, *Haidomyrmex scimitarus* (specimen
249 AMNH Bu-FB80) and *Linguamyrmex vladi* (specimen AMNH BuPH-1) were scanned at
250 the American Museum of Natural History Microscopy and Imaging Facility using a GE

251 phoenix vltomelx s240 60kV CT-scanner. Specimen AMNH Bu-FB80 was imaged at
252 180 μ A for 5 second exposures and a voxel size of $\sim 8\mu\text{m}$; specimen AMNH BuPH-1 at
253 250 μ A for 1 second exposures and a voxel size of $\sim 3\mu\text{m}$. The *Pseudomyrmex macrops*
254 specimen (AMNH DR-14-1021) was imaged at the New Jersey Institute of Technology
255 York Center using a Bruker SkyScan 1275 at 60kV and 150 μ A for 1 second exposures
256 with a subsequent voxel size of $\sim 3.5\mu\text{m}$. Volume reconstruction of the x-ray images was
257 conducted in 3D Slicer v4.11 (Fedorov et al. 2012) using the Segmentation modules;
258 still images of the reconstructed specimens were subsequently imported into ImageJ
259 (Abràmoff et al. 2004) for linear measurements to retain consistency with
260 measurements taken under stereo microscopy.

261
262 Most hell ant traits were distinguished as homologous to extant species; however,
263 because haidomyrmecine cranial morphology is highly modified, eye position is difficult
264 to assess in the context of modern ant variation. Extant ants (and most extinct ants,
265 including the Dominican *Pseudomyrmex* fossil) have a prognathous head posture, in
266 which the long axis of the head is held parallel to the ground with the oral opening
267 pointing anteriad. In many other insect taxa, such as wasps and grasshoppers, the head
268 is held in a hypognathous posture; the long axis of the head is held perpendicular to the
269 ground, with the oral opening positioned ventrally. A hypognathous-like head posture is
270 also present in hell ants, a configuration not seen in any extant ant. This difference in
271 head posture means that, interpreted strictly on the basis of homology, the dorsoventral
272 axis of the extant ant head is the anteroposterior axis of the hell ant head, and vice
273 versa; that eye positioning along each axis is similarly swapped. When interpreted this
274 way, the eye position of the hell ant is more similar to many *Camponotus* species:
275 positioned extremely posteriorly and more dorsally.

276
277 Functionally, however, the hell ant would have been moving with its head held
278 hypognathously, as evidenced by fossilized posture as well as preserved predation
279 (Perrichot et al 2008; Barden & Grimaldi 2012; Perrichot et al. 2016; Barden et al. 2020)
280 thus the functional anteroposterior axis of the hell ant head would be from its clypeal
281 protrusion or horn to the occipital foramen, rather than the homologous anteroposterior
282 axis of the head running perpendicular to the ground from vertex to oral opening.
283 Considering that our question is a question of functional ecology - what is the ecological
284 occupation of hell ants? - we measured traits related to eye position both functionally
285 and homologously, to incorporate this possible variation.

286 Due to limitations measuring specimens directly from amber fossils, we produced two
287 fossil morphometric datasets: one 'incomplete dataset' which excluded a subset of traits
288 for all specimens; and one with all measurements included. The incomplete dataset
289 lacked the frontal head length, head width, frontal mandible length, and pronotal width

290 measurements. These measurements are often difficult to accurately capture because
291 amber fossils are typically prepared to expose a clear lateral profile of any inclusions,
292 leaving the dorsal and frontal margins of the amber curved and distorted. Twenty hell
293 ant specimens were included in this incomplete dataset.

294
295 The complete dataset comprised the proof-of-concept fossil *Pseudomyrmex macrops*
296 specimen and three hell ant specimens: *Dhagnathos autokrator*, *Haidomyrmex*
297 *scimitarus*, and *Linguamyrmex vladi*. While the majority of specimens were workers, two
298 of the specimens - the complete *Dhagnathos autokrator* and *Haidomyrmex scimitarus*
299 were represented by alate and dealate queens, respectively. We include these here for
300 two reasons: one, hell ant queens are hypothesized to have actively foraged and hunted
301 in early colony foundation, and so likely occupied a similar ecological niche to the
302 workers of the species; and two, worker specimens are limited in many hell ant species
303 and entirely absent in the genus *Dhagnathos*. While we have no comparison to
304 *Dhagnathos* workers, we include a *Haidomyrmex scimitarus* worker in the incomplete
305 morphometric dataset, allowing us to compare the accuracy of the model in predicting
306 alate and worker ecology. A full list of all specimens included with information pertaining
307 to their sampling methods and castes can be found in Table S6; all morphometric data
308 for fossil specimens may be found in Supplementary Data_Fossil Morphometrics.
309 To ensure that morphological diversity for traits measured from fossil species are within
310 the bounds of extant morphological diversity, we conducted principal component
311 analysis (PCA) to compare morphospace occupation of hell ants relative to extant
312 lineages. We conducted separate PCAs for both the raw measurements and size-
313 corrected ratio measurements. All PCAs were implemented in R packages “corrplot”
314 (Wei et al. 2017) and “FactoMineR” (Lê et al. 2008).

315

316 **Random Forest model implementation**

317 We implemented different sets of Random Forest models, given the missing traits in our
318 incomplete fossil dataset; once with the missing traits eliminated from the extant ant
319 morphometric training dataset, and once including all traits for the complete fossil
320 dataset. For each dataset, we implemented two models using the raw measurements
321 and the size-corrected ratio measurements. Using these two models, we predicted
322 ecological niche aspects of hell ants twice; once using functional morphology, and once
323 using homologous morphology. Thus, each specimen’s ecological niche was predicted
324 four times: using raw measurements with functional morphology, raw measurements
325 with homologous morphology, size-corrected ratio measurements with functional
326 morphology, and size-corrected ratio measurements with homologous morphology. We
327 compiled all posterior probabilities of each prediction into a heatmap of model

328 predictions for each specimen with the R package “ggplot2” (Wickham 2016) to better
329 visualize the consensus among models for each predicted ecological niche aspect.

330

331 ***Comparative ecomorphological niche occupation***

332 To assess the specificity and breadth of niche occupations in haidomyrmecines, we
333 generated three-dimensional ecomorphological matrices comprising living and extinct
334 predatory taxa. Our taxonomic sampling included five lineages: hell ants as well as all
335 four distantly related extant groups with trap-jaw like morphology and behavior, wherein
336 workers act as solitary hunters that capture prey; many, but not all, do so through rapid
337 closure of specialized mandibles (Gronenberg and Ehmer 1996, Hölldobler & Wilson
338 1990). While the speed of prey capture is not known in hell ants, haidomyrmecines are
339 united with some extant trap jaw taxa by the presence of elongate setae (interpreted as
340 trigger hairs) in the path of mandible closure and dramatic morphological adaptations
341 related to predation (Dlussky 1996; Barden & Grimaldi 2012; Perrichot et al. 2016;
342 Barden et al. 2017). Importantly, all species within our sampling are primarily solitary
343 hunters (Larabee et al. 2014; Barden et al. 2020) in contrast to group raiding or
344 collective prey capture that typify many other predatory ant lineages (Dornhaus &
345 Powell 2010). Trap jaw mechanisms have evolved at least ten times in living ants
346 (Larabee et al. 2014; Booher et al. 2021); these origins are distributed among four
347 monophyletic lineages. Extant trap jaw predation has evolved once within each of the
348 subfamilies Ponerinae and Formicinae, thus our sampling included species within
349 relevant genera: *Anochetus* + *Odontomachus* and *Myrmoteras*, respectively. There are
350 at least eight trap jaw origins within the subfamily Myrmicinae and seven of these have
351 occurred within the genus *Strumigenys*. Our myrmicine sampling therefore included
352 *Strumigenys* as well as the five “dacetine” trap-jaw genera: *Acanthognathus*, *Daceton*,
353 *Epopostruma*, *Microdaceton*, and *Orectognathus*. Although it is not yet clear whether all
354 dacetine trap jaws are the product of a single origin, we grouped these taxa in analyses
355 as they are more closely related to each other than any are to *Strumigenys* (Ward et al.
356 2015).

357

358 To estimate the total number of unique ecomorphological combinations for each
359 specialized predatory lineage, we gathered niche occupation and size data for a total of
360 982 species, including 15 hell ant species with ecologies estimated under random
361 forest. Our extant sampling represents a minimum of 50% species sampling for each
362 genus. Each species was assigned one of three foraging and three nesting niche
363 aspects according to our modeling results for haidomyrmecines or published natural
364 history observations for extant taxa (Supplementary Data_Trapping Ecomorphospace).
365 Because observational data do not exist for all species, we applied published
366 generalizations in some cases (e.g. *Strumigenys* are noted as almost always leaf litter

367 nesting and foraging, we assumed this occupation by default except when otherwise
368 noted in the literature).

369

370 To estimate body size, we gathered minimum and maximum Weber's length (a
371 measurement of mesosoma length and traditional metric of ant size) measurements
372 from taxonomic descriptions and revisions. To include taxa without published
373 morphometric data, we collected Weber's length measurements from publicly available
374 images on AntWeb (AntWeb 2021) using ImageJ. We discretized species sizes by
375 delimiting Weber's length ranges for each species into at least one of twelve equal size
376 binnings. Size binning ranges were defined as one half of the standard deviation of
377 Weber's length measurements across all species. In cases where a species Weber's
378 length range exceeded any one size binning, we assigned multiple size binnings for that
379 species.

380

381 We generated three-dimensional ecological disparity values for each lineage following a
382 modification of Chen et al. (2019). We assigned each ecological binning a numerical
383 value from 1 to 3 based on inferred ecological proximity (nesting niche: leaf litter = 1,
384 ground = 2, lignicolous = 3; foraging niche: leaf litter = 1, epigaeic = 2, arboreal = 3),
385 while values for the third ecological dimension, body size, were continuous from 1 to 12.
386 To reduce the impact of species sampling bias between fossil and extant lineages, we
387 calculated disparity only among unique occupations, not between species. We created
388 a matrix of unique niche occupations for each lineage and calculated intra-lineage
389 disparity values by summing the distances between niche aspects for all pairwise
390 combinations of unique occupations using the equation. For example, the ecological
391 disparity between unique occupation 1 (uo_1) and unique occupation 2 (uo_2) would be: $|$
392 Nesting Niche $_{uo_1}$ - Nesting Niche $_{uo_2}$ $|$ + $|$ Foraging Niche $_{uo_1}$ - Foraging Niche $_{uo_2}$ $|$ + $|$
393 Body Size $_{uo_1}$ - Body Size $_{uo_2}$ $|$. We summarized mean and standard deviations for each
394 lineage using ggplot. Visual representations of lineage specific ecomorphological
395 occupations (ecospaces) were generated using the R package "rgl" (Adler et al. 2021)
396 and redrawn in Adobe Illustrator.

397

398 **Results**

399 *Model performance and prediction sensitivity*

400 Visualization of extant and extinct morphospace through principal component analysis
401 illustrated that extinct morphospace fully overlaps with extant morphospace
402 representing raw trait measurements, and mostly overlaps with extant morphospace
403 representing size-corrected ratio measurements (Supplemental Figures S3, S4).

404 Although hell ant morphology is distinct, the hell ant morphospace represented by
405 measurements incorporated in our models is primarily within the bounds of extant

406 diversity. Principal component 1 in the size-corrected ratio morphospace is primarily
407 driven by mandible size relative to body size, which is greater in many hell ants
408 compared to extant ants, likely resulting in the small portion of unique hell ant
409 morphospace. Predictions from size-corrected ratio measurements are often not
410 significantly different from predictions using raw measurements, however, and this
411 along with a great degree of morphospace overlap suggests that extant morphology is
412 an appropriate analog for extinct ecomorphology.

413
414 The fossil *Pseudomyrmex macrops* specimen used as a proof-of-concept was
415 consistently and accurately predicted as a lignicolous arboreal-foraging phytophagivore
416 (Figure 2). The arboreal foraging niche was predicted with the highest confidence, while
417 the phytophagous functional role was predicted with the lowest confidence (Tables S7-
418 S22). This specimen was preserved in Dominican amber, approximately 16 Ma, and
419 measurements were taken from a microCT scan: the accuracy of the model prediction
420 suggests that neither taphonomy nor microCT scan-based measurements distort
421 morphology in prediction.

422
423 Hell ants are primarily recovered as epigaeic foragers that nested directly in the ground,
424 though several species are predicted as leaf litter nesters and foragers (Figure 2).
425 Additionally, one *Haidomyrmex* morphospecies (*Haidomyrmex sp3*) was partially
426 predicted as a lignicolous nester and arboreal forager; with *Linguamyrmex brevicornis*
427 also partially predicted as an arboreal forager. Hell ants were primarily predicted as
428 predators, both specialist and generalist, though some species were additionally
429 predicted to be omnivorous (Figure 2, Supplemental Tables S7-S38). Given the
430 ecological plasticity in many extant ant species - many species are primarily predaceous
431 but may supplement their diet with plant material - we may expect hell ants to follow this
432 same pattern. Additionally, even when species were predicted as omnivores, the
433 probabilities of specialist predation and generalist predation when summed were greater
434 than the probability of omnivory, suggesting that atomization of predator classes may
435 have played some role in the prediction of omnivory. Supporting the general accuracy of
436 our models, we find broad congruence across species and also do not recover any
437 strong predictions of unlikely ecological niches: hell ants were not predicted as
438 subterranean nesters, column-raiding foragers, or fungivorous, granivorous, or
439 phytophagous functional roles (Figure 2).

440
441 Posterior probabilities for each prediction (an indicator of Random Forest model vote
442 consensus) were highest with foraging niche and nesting niche predictions, indicating
443 overall greater confidence in these predictions (Figure 2, Supplemental Tables S7-S38).
444 Predictions for functional role and ecomorph had lower posterior probabilities (Figure 2,

445 Supplemental Tables S7-S38). This may be a function of a greater number of potential
446 aspects for each (six possible functional roles and ten possible ecomorphs), necessarily
447 splitting the model votes. Extant morphology may also have less predictive power for
448 extinct ecology with respect to functional role and ecomorph, resulting in lower
449 predictive accuracy.

450

451 Intraspecific consensus among the four models used was variable. For some
452 specimens, there was very strong agreement, with all four models predicting the same
453 ecological niche aspect binning; however, there were also cases where two models
454 predicted one niche aspect binning, and two predicted another (Figure 2, Supplemental
455 Tables S7-S38). There were rarely scenarios where more than two niche aspect
456 binnings were predicted for a single specimen. More frequently in situations of evenly
457 split predictions, the size-corrected ratio models would predict the same aspect binning
458 while the raw measurement models would predict another; this suggests that the
459 difference between functional morphology and homologous morphology with respect to
460 eye positioning did not matter as much to niche prediction. This may be because the
461 model ranked eye positioning traits relatively low on its scale of variable importance,
462 thus, the difference between functional and homologous morphology was negligible
463 (Supplemental Figure S4, S5).

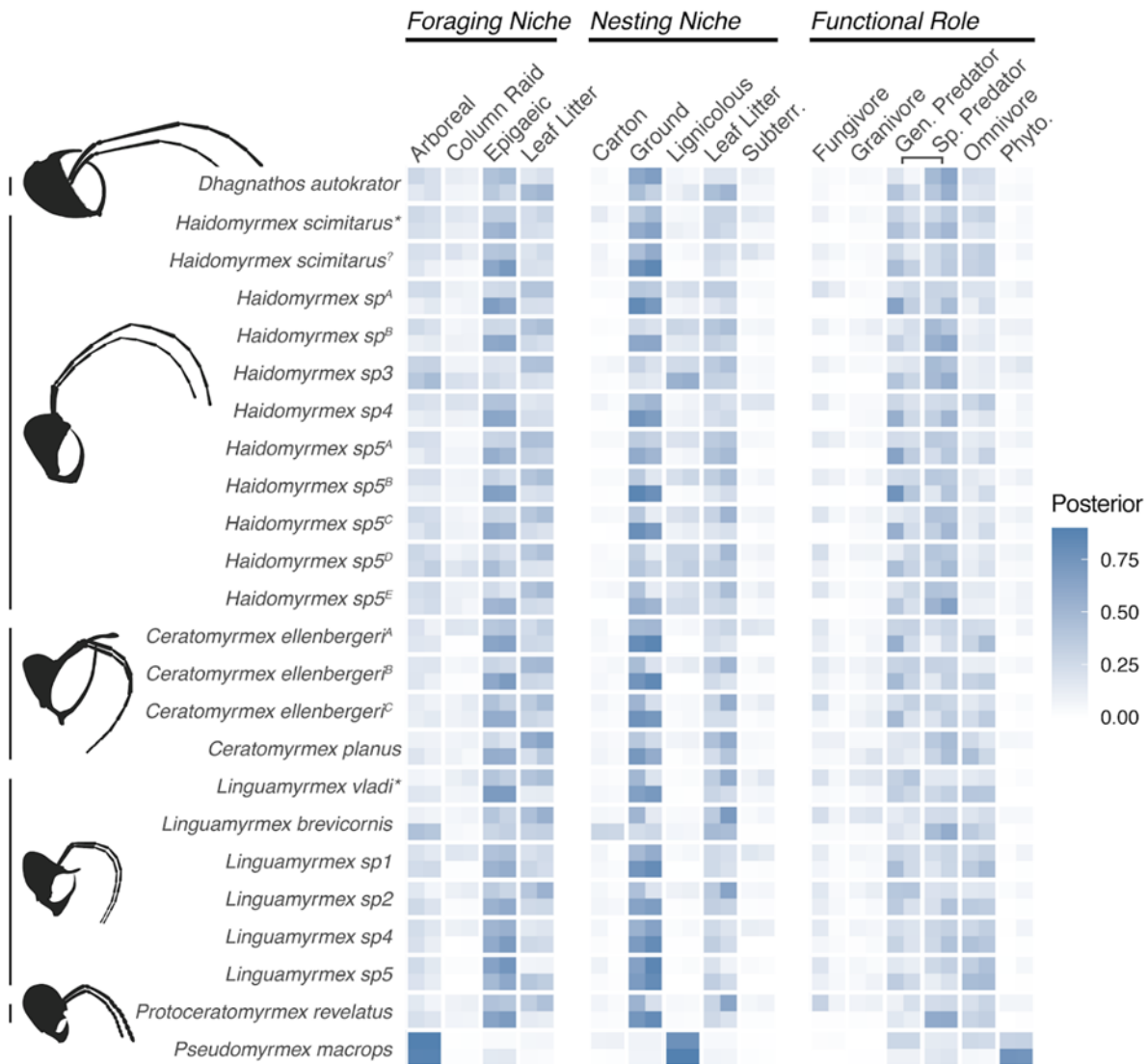
464

465 There was a limited drop in accuracy from the models trained on the full
466 morphometric dataset to the models trained on the limited morphometrics dataset, with
467 missing traits removed (Table S5). In most cases, the difference was only a few
468 percentage points, at most five percent. This limited decrease in accuracy suggests that
469 the traits removed were not essential to be measured, and that there is a core set of
470 most relevant traits. Variable importance plots from the models rank traits related to
471 eyes, antennae, legs, and mandibles as most crucial to model accuracy (Supplemental
472 Figures S5, S6). The traits that were removed primarily dealt with dimensions of the
473 head and thorax; while their inclusion improves model accuracy, it is not necessary to
474 include all of them in order to obtain a reasonably accurate prediction of extinct
475 ecological niches.

476

477 We found no robust differences in niche predictions between specimens
478 measured directly and microCT-measured specimens; specimens measured from
479 microCT scans were also predicted as epigaeic or leaf litter foragers and nesters
480 (Figure 2, Tables S7-S38). Additionally, we find that the dealate *Haidomyrmex*
481 *scimitarus* (measured from a microCT scan) and the worker *Haidomyrmex scimitarus*
482 (measured through light microscopy) were both predicted to be ground-nesting epigaeic
483 predators (Figure 2, Supplemental Tables S7-S38); illustrating consensus between the

484 two types of input data. This congruent ecological assignment also supports the
 485 hypothesis that stem-ant queens did not establish nests through claustral founding –
 486 queens of many extant species do not actively forage themselves – but occupied the
 487 same general ecological niche as workers of their species (Barden & Grimaldi 2012).
 488



489 **Figure 2.** Posterior probabilities of niche aspect predictions. Each species' niche aspect
 490 predictions are represented by four models derived from alternate datasets; from top
 491 left, clockwise: raw functional measurements, raw homologous measurements, size-
 492 corrected ratio functional measurements, size-corrected ratio homologous
 493 measurements. Taxonomic sampling includes described (named) taxa as well as
 494

495 putative morphospecies. Alternate specimens of the same species are denoted with
496 superscripts, *denotes specimens included through CT-scan reconstruction data. All
497 posterior probabilities are available in Supplemental Tables S7-38; full specimen
498 information is available in Supplemental Table 6.

499

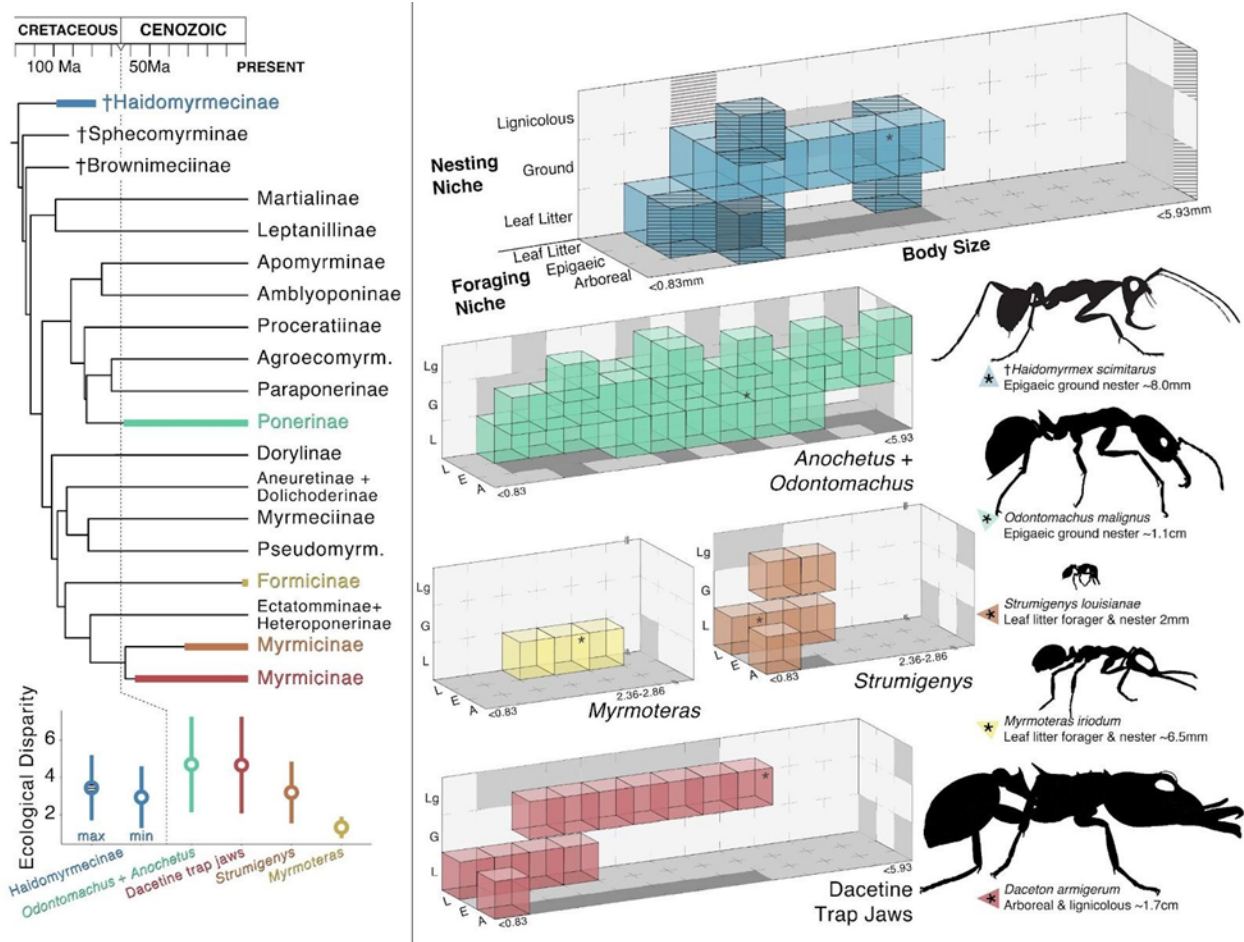
500 *Niche occupation in extinct and extant specialized predators*

501 Our most conservative estimates of ecological niche occupation suggest that hell ants
502 occupied primarily ground-nesting epigaeic niches with some leaf litter occupation, while
503 across-model results recover hell ants within arboreal, ground, and leaf litter niches
504 across a moderate body size range. In comparing predicted hell ant ecospace to solitary
505 predator ant ecospace, we find that hell ants occupied at least part of the
506 ecomorphological spaces occupied by extant lineages (Figure 3). The sister ponerine
507 genera *Anochetus* and *Odontomachus* exhibit the greatest extant ecospace diversity
508 and disparity, occupying most potential ecospace, with species ranging from ~3mm to
509 ~1.7cm spanning arboreal, ground, and leaf litter niches (Brown 1978; Hoenle et al.
510 2020). The most restricted ecospace is occupied by species within the formicine genus
511 *Myrmoteras*, which are minute leaf litter dwellers.

512

513 Ecological disparity does not appear to be linked to species diversity per se: the most
514 taxonomically diverse trapjaw lineage is *Strumigenys* with over 850 species, but the
515 constrained size and primarily leaf litter habits of the genus produce a within-group
516 ecological disparity that is low relative to *Anochetus* and *Odontomachus* with 188 total
517 species (Figure 3) (Bolton 2021). Similarly, while total species diversity of hell ants is
518 unknown, even within our limited fossil sample, haidomyrmecines are found to be
519 relatively ecologically disparate and diverse compared to extant lineages.

520



521
 522 **Figure 3.** Ecospace occupation of haidomyrmecine and extant specialist predator
 523 lineages. (Top left) Subfamily-level time-calibrated phylogeny of ants with divergence
 524 dates from Borowiec et al. (2019), Haidomyrmecinae and extant lineages denoted with
 525 colored bars; haidomyrmecine range derived from oldest and youngest deposit ages,
 526 extant ranges based on available crown age estimations for each lineage: Ponerinae –
 527 *Anochetus* + *Odontomachus* (Fernandes et al. 2021); Myrmicinae – *Strumigenys*
 528 (Booher et al. 2021); Myrmicinae – dacetine trap-jaws (Ward et al. 2015). No
 529 divergence date estimates are available for the formicine trap-jaw genus *Myrmoteras*.
 530 (Right) Lineage-specific ecomorphological niche occupations. Each colored cube
 531 represents a unique occupied niche. Hashed cubes in haidomyrmecine ecospace
 532 indicate “maximum” hypothetical niche occupation based on all unique combinations
 533 estimated across all four random forest models while remaining cubes reflect only the
 534 majority aspect from the raw functional measurement model. All extant ecospaces
 535 compiled from literature. (Bottom left) Within-lineage disparity calculated as average
 536 pairwise distance between each unique three-dimensional occupation. Maximum and

537 minimum haidomyrmecine values represent alternate niche occupations described in
538 the right panel. Disparity values are listed in Table S39.

539

540 **Discussion**

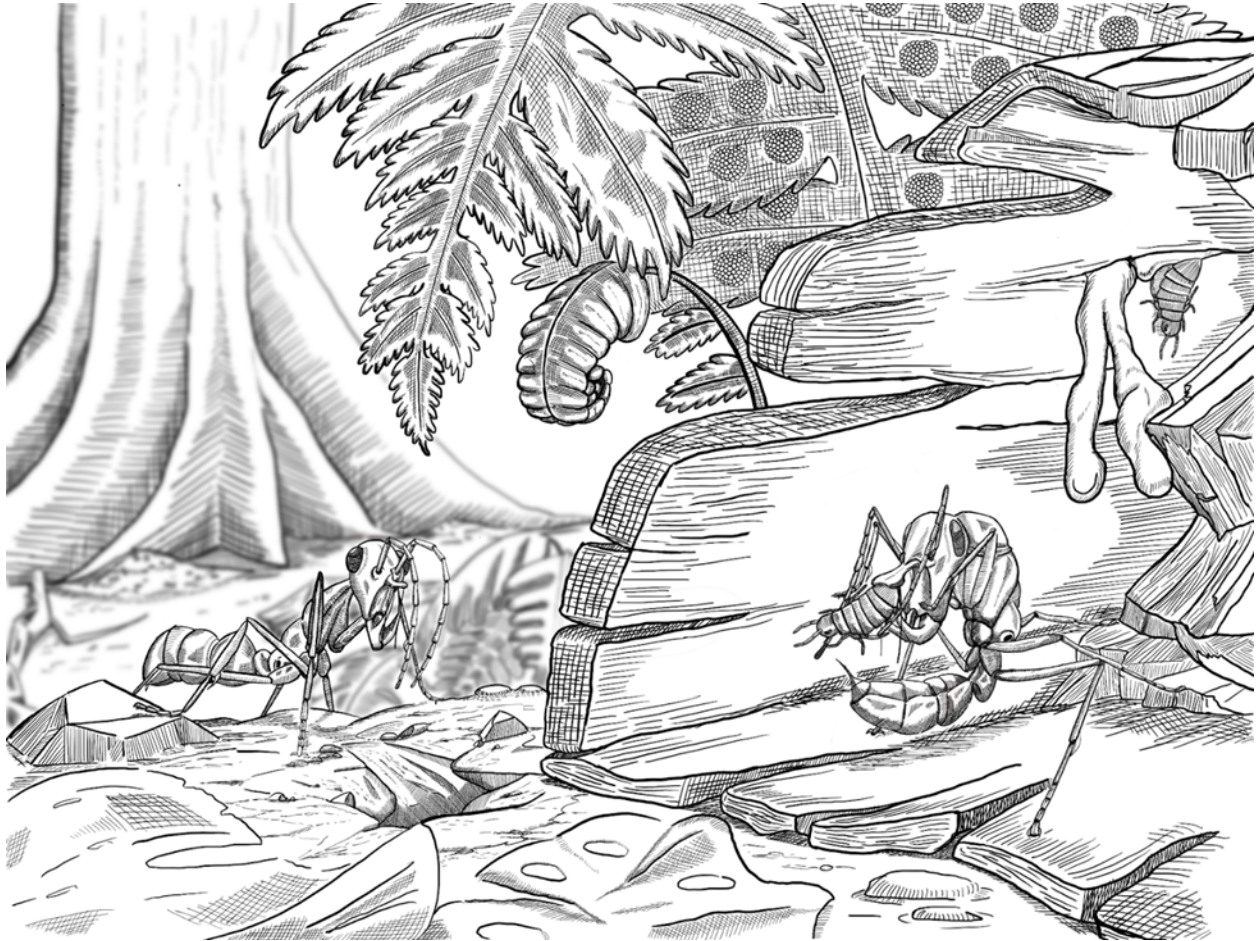
541 *Hell ants as epigaeic or leaf litter predators*

542 We recover broad consensus across models for hell ant ecological niche occupations:
543 models consistently predicted haidomyrmecine taxa as leaf litter foraging or epigaeic
544 ground-nesting predators, with few outliers (Figure 4). Variations within the testing
545 datasets, such as homologous vs functional morphology or missing traits, did not greatly
546 affect predictions. Our results are in contrast to previous hypotheses suggesting a
547 primarily arboreal lifestyle among hell ants. Initial hypotheses were based on qualitative
548 assessments of morphology (Barden & Grimaldi 2012) and an assertion that hell ants'
549 vertically aligned mandibles might have precluded the fine manipulation of soil required
550 to create ground nests (Dlussky 1996). However, extant and fossilized behavioral
551 evidence provide support for ground and leaf litter leaf litter habits among in
552 haidomyrmecines. Many extant trap-jaw ant species are capable of manipulating soil
553 with their highly specialized mandibles, allowing for nesting directly in the ground
554 (Cerquera & Tschinkel 2010). Soil nesting is also estimated as the ancestral state
555 among all crown ants, although fossils have not yet been included in such
556 reconstructions (Lucky et al. 2013). Additionally, two fossilized examples of hell ant prey
557 reflect leaf litter and surficial habitats: a beetle larva in association with a *Linguamyrmex*
558 *vlati* worker (Barden et al. 2017), likely reflecting a humid leaf litter habitat; and a
559 cockroach relative *Caputoraptor elegans* in association with *Ceratomyrmex ellenbergi*
560 (Barden et al. 2020), possibly living in leaf litter or surficial areas, although arboreal
561 habitats have been proposed (Bai et al. 2018). This reconstructed nesting ecology
562 aligns with proposed “extrinsic factors” related to the evolution of eusociality (Evans
563 1977).

564

565 Entrapment bias of ants in amber tends to skew towards arboreal species, though
566 preservation is contingent on the position of resin secretions on the source plant
567 (Solórzano-Kraemer et al. 2015, 2018). Experiments conducted using sticky traps as a
568 resin analogue found that sticky traps placed higher up in the trees collected arboreal
569 species, while traps placed within one meter of the ground collected leaf litter species,
570 possibly foraging for prey caught in the traps (Solórzano-Kraemer et al 2018). While we
571 do not recover hell ants primarily as arboreal species, it is possible that hell ants
572 foraging around the base of trees, perhaps attracted by struggling prey, would have
573 themselves become entrapped in amber. This may be similar to fossilization in asphalt
574 and tar traps, where predatory species are overrepresented because they are attracted
575 to dying prey animals trapped in the tar (Stock 2001). Considering the broad diversity of

576 specimens entrapped in Cretaceous amber (Sánchez-García and Engel 2016; Selden
577 and Ren 2017; Stoev et al. 2019; Yu et al. 2019; Ngô-Muller et al. 2020), it is likely that
578 at least some amber secretions occurred lower on trunks or root buttresses, entrapping
579 ecologically diverse segments of the overall amber biota. Additionally, evidence from
580 Cenozoic amber ant assemblages finds that ground-dwelling ant species are frequently
581 entrapped in resin, lending further support to the likelihood of entrapment for non-
582 arboreal hell ants (Guénard et al. 2015).
583



584
585 **Figure 4.** Reconstruction of the putative nesting and predatory foraging habits of the
586 hell ant *Linguamyrmex vladi*. Artist: John Paul Timonera.

587

588 *Ecospace occupation and ecological succession*

589 Many extant predatory ants hunt in groups, however some lineages capture prey alone
590 (Beckers et al. 1989) and certain morphological adaptations necessitate solo foraging.
591 Workers of extant trap-jaw ants capture prey through rapid closure of their specialized
592 mandibles – often a power-amplified mechanism is employed following the activation of
593 elongate trigger setae in the path of mandible movement. This specialized prey capture

594 typically precludes group predation; workers individually subdue a single prey item
595 before returning to the nest. An instance of preserved predation has demonstrated that
596 hell ants captured prey alone in a manner analogous to modern trap-jaw taxa (Barden
597 et al. 2020). Hell ant workers pinned prey between their vertically-expanded tusk-like
598 mandibles and cranial appendages. Our results suggest that hell ants may have been
599 functional equivalents to many modern-day trapjaws in surficial and leaf litter arthropod
600 communities; solitary foraging hunters seeking out prey across the forest floor and in
601 interstitial leaf litter spaces. While there are some morphological traits that support a
602 trap-jaw mechanism in hell ants, including trigger hairs and a structurally-reinforced
603 clypeal paddle at the point of mandible articulation, it is unknown whether or not hell
604 ants were trap-jaw predators. Nevertheless, they were most likely solitary-foraging
605 predators, considering fossil paleoethological evidence and consistent individual
606 fossilization of specimens, in contrast to worker aggregations known in other stem-ant
607 genera (Barden & Grimaldi 2016; Barden et al. 2020).

608
609 We recover a pattern of repeated ecological niche occupation across lineages of
610 solitary-foraging specialized ant predators. Even as molecular-based divergence
611 estimates place the origin of crown ants during the Cretaceous (Borowiec et al. 2019;
612 Moreau et al. 2006), the earliest extant trap-jaw predators originated in the Cenozoic
613 (Figure 3) (Booher et al. 2021; Fernandes et al. 2021; Ward et al. 2015). Molecular
614 divergence-date estimates for crown-group origins of trap-jaw lineages range from ~65
615 Ma in ponerine ants (Fernandes et al. 2021) to ~35 Ma in the myrmicine genus
616 *Strumigenys* (Booher et al. 2021). The last hell ant fossil dates to 78 Ma in Campanian
617 age Canadian amber (McKellar et al. 2013). It is unclear precisely when hell ants went
618 extinct, however it seems plausible that a mass extinction event may have contributed
619 to their demise. The overlap of ecospace occupation between hell ants and the lineages
620 arising soon after the Cretaceous-Paleogene extinction (KPg), ponerine and dacetine
621 trap jaw ants, suggests faunal turnover in niche occupation. The ecological breadth of
622 modern trap jaw ants may represent echoes of their Cretaceous counterparts.

623
624 Our reconstructed hell ant ecospace overlaps with occupations of all extant groups
625 sampled. Hell ants occupied approximately 10% of total potential sampled
626 ecomorphospace and radiated into arboreal, leaf litter, and surficial habitats.
627 Subsequently, other specialized predatory ant lineages radiated into ecomorphospace
628 that partially overlaps with hell ant ecomorphospace. Trap-jaw dacetines and ponerines
629 emerged relatively rapidly after the Cretaceous end extinction, while other trap-jaw
630 lineages emerged later in the Cenozoic; however, all lineages occupy at least part of the
631 hell ant ecomorphospace. This pattern illustrates potential ecological restriction of
632 solitary specialized predators. Additionally, while we included most known species in

633 extant ecospace reconstructions, our fossil sampling was much more limited; thus the
634 full ecospace occupation of hell ants was probably more broad than our current
635 reconstruction suggests.

636

637 *Pitfalls and potential of paleoecological niche reconstructions*

638 We present here a pipeline for paleoecological niche prediction using machine learning
639 algorithms and broad ecomorphological sampling. To our knowledge, this is the first
640 attempt at predicting extinct ecology using Random Forest. Because this class of
641 supervised machine learning incorporates non-linear modeling and has been shown to
642 outperform various other discriminant function methods (Pigot et al. 2020; Sosiak &
643 Barden 2021), it represents a powerful tool in reconstruction of fossil niche occupations
644 and communities. The method requires a taxonomic group with both fossil and extant
645 representatives, which exhibit consistent body plans, allowing for homologous trait
646 measurements across time series. The application of extant trait data in extinct
647 ecological estimation is best suited among lineages that exhibit a high degree of extant
648 diversity relative to fossil samples: the more ecologies that the extant group occupies,
649 the more likely it will be that all potential ecological niches of the extinct group are
650 represented.

651

652 Predicted ecologies may also be evaluated in the context of other fossil evidence. For
653 example, several extant ant taxa are primarily granivorous seed-eaters (Cole 1968;
654 Plowes et al. 2013), thus the functional role of extinct species could potentially be
655 predicted as granivorous. However, while grasses first evolved in the early Cretaceous,
656 grassland ecosystems did not develop broadly until later in the Cenozoic, making it
657 unlikely that Mesozoic ants would have been granivorous (Stromberg 2011; Boyce and
658 Lee 2017). Indeed, while our model allowed for six functional role binnings,
659 haidomyrmecines were never predicted as belonging to temporally inappropriate
660 ecologies with any certainty, even as our included Cenozoic fossil specimen was
661 correctly estimated as an uncommon phytophagivore.

662

663 Quantitative predictions of ecological niches allow for new approaches to many
664 paleoecological questions. We present here one such application; a relative comparison
665 of ecospace occupation between extinct and extant lineages. By reconstructing the
666 ecological community of the earliest ants, we find repeated lineage occupation of
667 ecospace, consistent with dynastic succession across Earth's last mass extinction
668 event.

669

670

671

672 **Acknowledgements**

673 We thank Christine Johnson and Christine Lebeau for facilitating access to specimens
674 at the American Museum of Natural History, in addition to Morgan Hill and Andrew
675 Smith for facilitating access to imaging equipment at the AMNH; Stefan Cover and
676 David Lubertazzi for facilitating specimen access and hospitality at the Museum of
677 Comparative Zoology; Eugenia Okonski and Ted Schultz for facilitating specimen
678 access and hospitality at the Smithsonian National Museum of Natural History; all of
679 whom without which we would not have been able to develop the initial model.

680

681 **Funding**

682 A portion of the initial work in collecting extant ant data and developing the model was
683 funded by an Arthur James Boucot Research Grant from the Paleontological Society
684 and startup funding from the New Jersey Institute of Technology.

685

686 **Data and materials availability**

687 All data and scripts needed to reproduce the analyses and evaluate the conclusions in
688 the paper are present in the paper and/or in the Supplementary Materials.

689

690 **Competing Interest Statement**

691 The authors declare that they have no competing interests.

692

693 **Contributions**

694 Conceptualization: CES, PB

695 Methodology: CES, PB

696 Data compilation and collection: CES, VP, TJ

697 Data visualization: CES, PB, JPT

698 Writing—original draft: CES, PB

699 Writing—review & editing: CES, PB, VP, TJ, JPT

700

701 **Ethics**

702 The fossil specimens used in this research are preserved primarily within Burmese
703 amber. We affirm that all specimens were acquired prior to June 2017, pursuant to the
704 proposed boycott of Burmese amber by the Society of Vertebrate Paleontologists
705 (Rayfield et al. 2020). Some specimens are located in a private collection, while others
706 are located in institutional museums: specimen repositories are indicated in the
707 Supplementary Information associated with this manuscript, and we have provided
708 photomicrographs of all specimens residing in a private collection. All data associated
709 with this manuscript are available as Supplementary Information, including all
710 morphometric measurements for privately-owned specimens.

711 **References**

- 712 Abràmoff, M. D., Magalhães, P. J., & Ram, S. J. (2004). Image processing with ImageJ.
713 *Biophotonics International*, 11(7), pp.36-42.
- 714 Adler, D., Murdoch, D., Nenandic, O., Urbanek, S., Chen, M., Gebhardt, A., Bolker, B.,
715 Csardi, G., Strzelecki, A., Senger, A., & R Core Team. (2021). Package “rgl”.
- 716 AntWeb. Version 8.64.2. California Academy of Science, online at
717 <https://www.antweb.org>. Accessed February 2021.
- 718 Bai, M., Beutel, R. G., Zhang, W., Wang, S., Hörnig, M., Gröhn, C., Yan, E., Yang, X., &
719 Wipfler, B. (2018). A new Cretaceous insect with a unique cephalo-thoracic scissor
720 device. *Current Biology*, 28(3), pp.438-443.
- 721 Barden, P., & Grimaldi, D. (2012). Rediscovery of the bizarre Cretaceous ant
722 *Haidomyrmex Dlussky* (Hymenoptera: Formicidae), with two new species. *American*
723 *Museum Novitates*, 2012(3755), 1-16.
- 724 Barden, P., & Grimaldi, D. A. (2016). Adaptive radiation in socially advanced stem-
725 group ants from the Cretaceous. *Current Biology*, 26(4), 515-521.
- 726 Barden, P., Herhold, H. W., & Grimaldi, D. A. (2017). A new genus of hell ants from the
727 Cretaceous (Hymenoptera: Formicidae: Haidomyrmecini) with a novel head structure.
728 *Systematic Entomology*, 42(4), 837-846.
- 729 Barden, P., Perrichot, V., & Wang, B. (2020). Specialized predation drives aberrant
730 morphological integration and diversity in the earliest ants. *Current Biology*, 30(19),
731 3818-3824.
- 732 Barton, P. S., Gibb, H., Manning, A. D., Lindenmayer, D. B., & Cunningham, S. A.
733 (2011). Morphological traits as predictors of diet and microhabitat use in a diverse
734 beetle assemblage. *Biological Journal of the Linnean Society*, 102, 301–310.
- 735 Beckers, R., Goss, S., Deneubourg, J. L., & Pasteels, J. M. (1989). Colony size,
736 communication, and ant foraging strategy. *Psyche*, 96(3-4), 239-256.
- 737 Benson, R. B., Campione, N. E., Carrano, M. T., Mannion, P. D., Sullivan, C., Upchurch,
738 P., & Evans, D. C. (2014). Rates of dinosaur body mass evolution indicate 170 million
739 years of sustained ecological innovation on the avian stem lineage. *PLoS Biology*,
740 12(5), e1001853.
- 741 Bolton, B. (2021). An online catalog of the ants of the world. Available from
742 <https://antcat.org>. (accessed July 2021)
- 743 Booher, D. B., Gibson, J. C., Liu, C., Longino, J. T., Fisher, B. L., Janda, M., Narula, N.,
744 Toulkeridou, E., Mikheyev, A. S., Suarez, A. V., & Economo, E. P. (2021). Functional
745 innovation promotes diversification of form in the evolution of an ultrafast trap-jaw
746 mechanism in ants. *PLoS biology*, 19(3), e3001031.
- 747 Borowiec, M. L., Rabeling, C., Brady, S. G., Fisher, B. L., Schultz, T. R., & Ward, P. S.
748 (2019). Compositional heterogeneity and outgroup choice influence the internal
749 phylogeny of the ants. *Molecular phylogenetics and evolution*, 134, 111-121.

- 750 Boyce, C. K., & Lee, J. E. (2017). Plant evolution and climate over geological
751 timescales. *Annual Review of Earth and Planetary Sciences*, 45, 61-87.
- 752 Brady, S. G., Schultz, T. R., Fisher, B. L., & Ward, P. S. (2006). Evaluating alternative
753 hypotheses for the early evolution and diversification of ants. *Proceedings of the*
754 *National Academy of Sciences*, 103(48), 18172-18177.
- 755 Breiman L. (2001). Random Forests. *Machine Learning*, 45, 5-32.
- 756 Brown Jr, W. L. (1978). Contributions toward a reclassification of the Formicidae. Part
757 VI. Ponerinae, tribe Ponerini, subtribe Odontomachiti. Section B. Genus *Anochetus*
758 and bibliography. *Studia Entomologica*, 20(1-4), 549-652.
- 759 Cerquera, L. M., & Tschinkel, W. R. (2010). The nest architecture of the ant
760 *Odontomachus brunneus*. *Journal of Insect Science*, 10(1), 64.
- 761 Chen, M., & Wilson, G. P. (2015). A multivariate approach to infer locomotor modes in
762 Mesozoic mammals. *Paleobiology*, 41(2), 280-312.
- 763 Chen, M., Strömberg, C. A., & Wilson, G. P. (2019). Assembly of modern mammal
764 community structure driven by Late Cretaceous dental evolution, rise of flowering
765 plants, and dinosaur demise. *Proceedings of the National Academy of Sciences*,
766 116(20), 9931-9940.
- 767 Cole, A. C., Jr. 1968. *Pogonomyrmex* harvester ants. A study of the genus in North
768 America. Knoxville, Tenn.: University of Tennessee Press, x + 222 pp. (page 38, Key
769 to North American species)
- 770 Dickson, B. V., Sherratt, E., Losos, J. B., & Pierce, S. E. (2017). Semicircular canals in
771 *Anolis* lizards: ecomorphological convergence and ecomorph affinities of fossil
772 species. *Royal Society open science*, 4(10), 170058.
- 773 Dlussky, G. M. (1996). Ants (Hymenoptera: Formicidae) from Burmese amber.
774 *Paleontological Journal*, 30, 449-454.
- 775 Dornhaus, A., & Powell, S. (2010). Foraging and defence strategies. In L. Lach, C. L.
776 Parr, K. L. Abbott (Eds.), *Ant ecology*, 210-230.
- 777 Drumheller, S. K., & Wilberg, E. W. (2020). A synthetic approach for assessing the
778 interplay of form and function in the crocodyliform snout. *Zoological Journal of the*
779 *Linnean Society*, 188(2), 507-521.
- 780 Dunn, R. H., Cooper, C., Lemert, J., Mironov, N., & Meachen, J. A. (2019). Locomotor
781 correlates of the scapholunar of living and extinct carnivorans. *Journal of morphology*,
782 280(8), 1197-1206.
- 783 Engel, M. S., & Grimaldi, D. A. (2005). Primitive new ants in cretaceous amber from
784 Myanmar, New Jersey, and Canada (Hymenoptera: Formicidae). *American Museum*
785 *Novitates*, 2005(3485), 1-24.
- 786 Ercoli, M. D., Prevosti, F. J., & Alvarez, A. (2012). Form and function within a
787 phylogenetic framework: locomotory habits of extant predators and some Miocene

- 788 Sparassodonta (Metatheria). *Zoological Journal of the Linnean Society*, 165(1), 224-
789 251.
- 790 Evans, H.E., 1977. Commentary: extrinsic versus intrinsic factors in the evolution of
791 insect sociality. *BioScience*, 27(9), pp.613-617.
- 792 Fedorov, A., Beichel, R., Kalpathy-Cramer, J., Finet, J., Fillion-Robin, J.C., Pujol, S.,
793 Bauer, C., Jennings, D., Fennessy, F., Sonka, M. and Buatti, J. (2012). 3D Slicer as
794 an image computing platform for the Quantitative Imaging Network. *Magnetic
795 Resonance Imaging*, 30(9),1323-1341.
- 796 Fernandes, I. O., Larabee, F. J., Oliveira, M. L., Delabie, J. H., & Schultz, T. R. (2021).
797 A global phylogenetic analysis of trap-jaw ants, *Anochetus* Mayr and *Odontomachus*
798 *Latreille* (Hymenoptera: Formicidae: Ponerinae). *Systematic Entomology*, 46, 685-
799 703.
- 800 Figueirido, B., Martín-Serra, A., & Janis, C. M. (2016). Ecomorphological determinations
801 in the absence of living analogues: the predatory behavior of the marsupial lion
802 (*Thylacoleo carnifex*) as revealed by elbow joint morphology. *Paleobiology*, 42(3),
803 508-531.
- 804 Figueirido, B., Palmqvist, P., Perez-Claros, J. A., & Janis, C. M. (2019). Sixty-six million
805 years along the road of mammalian ecomorphological specialization. *Proceedings of
806 the National Academy of Sciences of the United States of America*, 116, 12698–
807 12703.
- 808 Frederickson, J. A., Engel, M. H., & Cifelli, R. L. (2018). Niche partitioning in theropod
809 dinosaurs: Diet and habitat preference in predators from the Uppermost Cedar
810 Mountain Formation (Utah, USA). *Scientific reports*, 8(1), 1-13.
- 811 Gerry, S. P., Wang, J., & Ellerby, D. J. (2011). A new approach to quantifying
812 morphological variation in bluegill *Lepomis macrochirus*. *Journal of Fish Biology*, 78,
813 1023–1034.
- 814 Gibb, H., Stoklosa, J., Warton, D. I., Brown, A. M., Andrew, N. R., & Cunningham, S. A.
815 (2015). Does morphology predict trophic position and habitat use of ant species and
816 assemblages?. *Oecologia*, 177(2), 519-531.
- 817 Grimaldi, D., & Agosti, D. (2000). A formicine in New Jersey Cretaceous amber
818 (Hymenoptera: Formicidae) and early evolution of the ants. *Proceedings of the
819 National Academy of Sciences*, 97(25), 13678-13683.
- 820 Gronenberg, W., & Ehmer, B. (1996). The mandible mechanism of the ant genus
821 *Anochetus* (Hymenoptera, Formicidae) and the possible evolution of trap-jaws.
822 *Zoology*, 99(3), 153-162.
- 823 Guénard, B., Perrichot, V. and Economo, E.P., (2015). Integration of global fossil and
824 modern biodiversity data reveals dynamism and stasis in ant macroecological
825 patterns. *Journal of Biogeography*, 42(12), pp.2302-2312.

- 826 Hertel, F. (1995). Ecomorphological indicators of feeding behavior in recent and fossil
827 raptors. *The Auk*, 112(4), 890-903.
- 828 Hoenle, P. O., Lattke, J. E., Donoso, D. A., von Beeren, C., Heethoff, M., Schmelzle, S.,
829 Argoti, A., Camacho, L., Ströbel, B., & Blüthgen, N. (2020). *Odontomachus davidsoni*
830 sp. Nov. (Hymenoptera, Formicidae), a new conspicuous trap-jaw ant from Ecuador.
831 *ZooKeys*, 948, p.75.
- 832 Hölldobler, B., & Wilson, E. O. (1990). *The Ants*. Harvard University Press.
- 833 Jenkins, X. A., Pritchard, A. C., Marsh, A. D., Kligman, B. T., Sidor, C. A., & Reed, K. E.
834 (2020). Using manual ungual morphology to predict substrate use in the
835 Drepanosauromorpha and the description of a new species. *Journal of Vertebrate*
836 *Paleontology*, 40(5), e1810058.
- 837 Lattke, J. E., & Melo, G. A. (2020). New haidomyrmecine ants (Hymenoptera:
838 Formicidae) from mid-Cretaceous amber of Northern Myanmar. *Cretaceous*
839 *Research*, 114, 104502.
- 840 Larabee, F. J., & Suarez, A. V. (2014). The evolution and functional morphology of trap-
841 jaw ants (Hymenoptera: Formicidae). *Myrmecological News*, 20, 25-36.
- 842 Lê, S., Josse, J., & Husson, F. (2008). FactoMineR: An R package for multivariate
843 analysis. *Journal of Statistical Software*, 25(1), 1–18.
- 844 Liaw, A., & Wiener, M. (2018). RandomForest: Breiman and Cutler's random forests for
845 classification and regression. R package version 4.
- 846 Losos, J. B. (1992). The evolution of convergent structure in Caribbean Anolis
847 communities. *Systematic Biology*, 41(4), 403–420
- 848 Lucky, A., Trautwein, M. D., Guenard, B. S., Weiser, M. D., & Dunn, R. R. (2013).
849 Tracing the rise of ants-out of the ground. *PLOS one*, 8(12), e84012.
- 850 Lungmus, J. K., & Angielczyk, K. D. (2021). Phylogeny, function and ecology in the
851 deep evolutionary history of the mammalian forelimb. *Proceedings of the Royal*
852 *Society B*, 288(1949), 20210494.
- 853 McKellar, R. C., Glasier, J. R., & Engel, M. S. (2013). A new trap-jawed ant
854 (Hymenoptera: Formicidae: Haidomyrmecini) from Canadian Late Cretaceous amber.
855 *The Canadian Entomologist*, 145(4), 454-465.
- 856 Meloro, C., & Louys, J. (2014). Ecomorphology of radii in Canidae: Application to
857 fragmentary fossils from Plio-Pleistocene hominin assemblages. *Acta*
858 *Palaeontologica Polonica*, 60(4), 795-806.
- 859 Meng, Q. J., Grossnickle, D. M., Liu, D., Zhang, Y. G., Neander, A. I., Ji, Q., & Luo, Z.
860 X. (2017). New gliding mammaliaforms from the Jurassic. *Nature*, 548(7667), 291-
861 296.
- 862 Moreau, C. S., Bell, C. D., Vila, R., Archibald, S. B., & Pierce, N. E. (2006). Phylogeny
863 of the ants: diversification in the age of angiosperms. *science*, 312(5770), 101-104.

- 864 Moreau, C. S., & Bell, C. D. (2013). Testing the museum versus cradle tropical
865 biological diversity hypothesis: phylogeny, diversification, and ancestral
866 biogeographic range evolution of the ants. *Evolution*, 67(8), 2240-2257.
- 867 Ngô-Muller, V., Garrouste, R., Pouillon, J. M., & Nel, A. (2020). A new micropterigid
868 moth from the mid-Cretaceous Burmese amber (Insecta: Lepidoptera). *Cretaceous*
869 *Research*, 109, 104375.
- 870 Palmqvist, P., Gröcke, D. R., Arribas, A., & Farina, R. A. (2003). Paleoecological
871 reconstruction of a lower Pleistocene large mammal community using
872 biogeochemical ($\delta^{13}\text{C}$, $\delta^{15}\text{N}$, $\delta^{18}\text{O}$, Sr: Zn) and ecomorphological approaches.
873 *Paleobiology*, 29(2), 205-229.
- 874 Perrichot, V., Lacau, S., Néraudeau, D., & Nel, A. (2008). Fossil evidence for the early
875 ant evolution. *Naturwissenschaften*, 95(2), 85-90.
- 876 Perrichot, V., Wang, B., Engel, M.S. (2016) Extreme morphogenesis and ecological
877 specialization among Cretaceous basal ants. *Current Biology*, 26(11): 1468-1472.
- 878 Pigot, A. L., Sheard, C., Miller, E. T., Bregman, T. P., Freeman, B. G., Roll, U., Seddon,
879 N., Trisos, C. H., Weeks, B. C., & Tobias, J. A. (2020). Macroevolutionary
880 convergence connects morphological form to ecological function in birds. *Nature*
881 *Ecology & Evolution*, 4(2), pp.230-239.
- 882 Plowes, N.J.R., Johnon, R.A. & Holldobler, B. 2013. Foraging behavior in the ant genus
883 *Messor* (Hymenoptera: Formicidae: Myrmicinae). *Myrmecological News* 18, 33-49.
- 884 R Core Team. (2021). R: A language and environment for statistical computing. R
885 Foundation for Statistical Computing.
- 886 Rayfield, E. J., Theodor, J. M. & Polly, P. D. (2020). Fossils from conflict zones and
887 reproducibility of fossil-based scientific data. *Society of Vertebrate Paleontology*
888 (SVP), letter, 21/04/2020. <https://vertpaleo.org/Society-News/SVP-Paleo-News/Society-News,-Press-Release/On-Burmes-Amber-and-Fossil-Repositories-SVPMemb.aspx>.
- 891 Rector, A. L., & Vergamini, M. (2018). Forelimb morphology and substrate use in extant
892 Cercopithecidae and the fossil primate community of the Hadar sequence, Ethiopia.
893 *Journal of human evolution*, 123, 70-83.
- 894 Sánchez-García, A., & Engel, M. S. (2016). Springtails from the Early Cretaceous
895 amber of Spain (Collembola: Entomobryomorpha), with an annotated checklist of
896 fossil Collembola. *American Museum Novitates*, 2016(3862), 1-47.
- 897 Saunders, M. B., & Barclay, R. M. R. (1992). Ecomorphology of insectivorous bats: A
898 test of predictions using two morphologically similar species. *Ecology*, 73(4), 1335–
899 1345.
- 900 Selden, P. A., & Ren, D. (2017). A review of Burmese amber arachnids. *The Journal of*
901 *Arachnology*, 45(3), 324-343.

- 902 Solórzano Kraemer, M. M., Kraemer, A. S., Stebner, F., Bickel, D. J., & Rust, J. (2015).
903 Entrapment bias of arthropods in Miocene amber revealed by trapping experiments in
904 a tropical forest in Chiapas, Mexico. *PLoS one*, 10(3), e0118820.
- 905 Solórzano Kraemer, M. M., Delclòs, X., Clapham, M. E., Arillo, A., Peris, D., Jäger, P.,
906 Stebner, F., & Peñalver, E., 2018. Arthropods in modern resins reveal if amber
907 accurately recorded forest arthropod communities. *Proceedings of the National
908 Academy of Sciences*, 115(26), 6739–6744.
- 909 Sosiak, C. E., & Barden, P. (2021). Multidimensional trait morphology predicts ecology
910 across ant lineages. *Functional Ecology*, 35(1), 139-152.
- 911 Stock, C. (2001). *Rancho La Brea: A record of Pleistocene life in California*, revised J.M.
912 Harris., Natural History Museum of Los Angeles, Science Series no. 37, pp. 113
- 913 Stoev, P., Moritz, L., & Wesener, T. (2019). Dwarfs under dinosaur legs: a new
914 millipede of the order Callipodida (Diplopoda) from Cretaceous amber of Burma.
915 *ZooKeys*, 841, 79.
- 916 Strauss, R. E. (2010). Discriminating groups of organisms. In *Morphometrics for
917 nonmorphometricians* (ed. AmtElewa), pp. 73–91. Berlin, Germany: Springer.
- 918 Strömberg, C. A. (2011). Evolution of grasses and grassland ecosystems. *Annual
919 review of Earth and planetary sciences*, 39, 517-544.
- 920 Ward, P. S., Brady, S. G., Fisher, B. L., & Schultz, T. R. (2015). The evolution of
921 myrmicine ants: phylogeny and biogeography of a hyperdiverse ant clade
922 (Hymenoptera: Formicidae). *Systematic Entomology*, 40(1), 61-81.
- 923 Wei, T., Simko, V., Levy, M., Xie, Y., Jin, Y., & Zemla, J. (2017). Package ‘corrplot’.
924 *Statistcian*, 56, 316–324.
- 925 Weiser, M. D., & Kaspari, M. (2006). Ecological morphospace of New World ants.
926 *Ecological Entomology*, 31(2), 131-142.
- 927 Wickham H (2016). *ggplot2: Elegant Graphics for Data Analysis*. Springer-Verlag New
928 York. ISBN 978-3-319-24277-4, <https://ggplot2.tidyverse.org>.
- 929 Williams, E. E. (1972). 3. The Origin of Faunas. Evolution of lizard congeners in a
930 complex island fauna: A trial analysis. In T. Dobzhansky, M. K. Hecht, & W. C. Steere
931 (Eds.), *Evolutionary Biology* (pp. 47–89), Meredith Corporation. Refer page 72
- 932 Wilson, E. O., Carpenter, F. M., & Brown, W. L. (1967). The first Mesozoic ants.
933 *Science*, 157(3792), 1038-1040.
- 934 Wilson, E. O. (1987). Causes of ecological success: the case of the ants. *Journal of
935 Animal Ecology*, 56(1), 1-9.
- 936 Wilson, E. O. (1987). The earliest known ants: an analysis of the Cretaceous species
937 and an inference concerning their social organization. *Paleobiology*, 13(1), 44-53.
- 938 Wilson, E. O., & Hölldobler, B. (2005). The rise of the ants: a phylogenetic and
939 ecological explanation. *Proceedings of the National Academy of Sciences*, 102(21),
940 7411-7414.

- 941 Yates, M. L., Andrew, N. R., Binns, M., & Gibb, H. (2014). Morphological traits:
942 Predictable responses to macrohabitats across a 300 km scale. PeerJ, 2, e271.
943 <https://doi.org/10.7717/peerj.271>
- 944 Yates, M., & Andrew, N. R. (2011). Comparison of ant community composition across
945 different land-use types: Assessing morphological traits with more common methods.
946 Australian Journal of Entomology, 50(2), 118-124.
- 947 Yu, T., Kelly, R., Mu, L., Ross, A., Kennedy, J., Broly, P., Xia, F., Zhang, H., Wang, B.,
948 & Dilcher, D. (2019). An ammonite trapped in Burmese amber. Proceedings of the
949 National Academy of Sciences, 116(23), pp.11345-11350.